DOI: 10.2478/cdem-2023-0010 CHEM DIDACT ECOL METROL. 2023;28(1-2):171-178

Tayeb SAOUD[1,2], Said BENRAMACHE[1,2*] and Abdallah DIHA[3]

# THE EFFECT OF Co AND Cu CO-DOPING ZnO THIN FILMS ON STRUCTURAL AND OPTICAL PROPERTIES

**Abstract:** Using a spray pneumatic technique, cobalt (Co) and copper (Cu) co-doped zinc oxide thin films were effectively deposited on a glass substrate. The goal of this work was to create a semiconductor with good optical and electrical properties by co-doping ZnO thin films with Cu and Co. The ZnO thin films obtained from the Co and Cu co-doping exhibit patterns of x-ray diffraction spectra that suggest they are hexagonal ZnO (wurtzite, JCPDS 36-1451). The thin film elaborated with 2 % Co and 7 % Cu has the lowest value of crystallite size ($D$ = 14.67 nm). The transmission spectra demonstrate that all films have good optical transparency in the visible spectrum, with 7 % Cu achieving the highest transmission. Increasing Cu contents raised the band gap energy. The value at the minimum was 3.31 eV. The optical band gap's broadening is a significant characteristic of advanced materials and may be useful in applications involving metal oxide nanostructures for visible light gas sensing.

**Keywords:** ZnO, thin films, Co and Cu co-doping, TCO spray pneumatic method

## Introduction

Zinc oxide is a naturally occurring semiconductor with a 3.37 eV direct band gap and a massive exciton binding energy of 60 meV. ZnO is an important semiconductor material due to its increasingly popular importance in scientific researches [1, 2]. ZnO has been widely employed in a variety of fields, including automobile manufacturing, medical equipment, interactions, computers, electronics, optoelectronics, biological materials, storing data, converting energy, as well as architecture. All previous applications indicate that ZnO it has unique features [1-7]. It is critical to determine which element or elements ZnO must be doped with in order to control the bands gap, conductivity, carrier's concentration and applications. Because of the potential uses in spintronics, several researchers have recently focused on doping levels ZnO with incorporating transition metals (TMs) such as Co, Mn, Cu, Ni, Fe, and Cr [1-10]. Copper is nearly optimal for changing the properties of ZnO among the other doping elements due to the atoms of copper possesses a radius and electronic shell similar to zinc atoms; thus, replacing zinc with copper does not result in a modification in the lattice constant. The influence of copper

[1] Materials, Energy and Environment Laboratory, University of Biskra 07000, Algeria, email: faroune.tayeb@gmail.com, benramache.said@gmail.com, ORCID: TS 0009-0006-0924-1208, SB 0000-0003-3343-6268
[2] Material Sciences Department, Faculty of Science, University of Biskra 07000, Algeria
[3] Mechanics Department, Faculty of Technology, Tebessa University, 12000, Tebessa, Algeria, email: diha_a@yahoo.fr, ORCID: AD 0000-0002-9059-0790
[*] Corresponding author: benramache.said@gmail.com

doping on the magnetic fields, photoluminescence, crystalline structure, transmittance, and band gap of ZnO films produced through magnetron sputtering RF, magnetron sputtering DC, pulsed laser deposition, sol-gel methods and spray pyrolysis, it has been extensively studied [8-15].

The goal of this work is to create a semiconductor with good optical and structural properties from Co and Cu co-doped ZnO thin films. The influence of various Co and Cu levels on the crystalline structure, transmittance, and optical energy of Co and Cu co-doped ZnO thin films has been examined. ZnO thin films were sprayed on a glass substrate utilising a spray pneumatic method at a temperature of 400 °C with sprayed rate of 2 mL/min.

## Materials and methods

The thin films of $Zn_{1-(0.02+y)}Co_{0.02}Cu_yO$ thin films were sprayed utilising the spray pyrolysis method on glass substrates (GS). The solution preparation was dissolved by zinc acetate ($Zn(CH_3CO_2)_2$, $2H_2O$) in distilled water to form a 0.1 M solution with cobalt chloride ($CoCl_2$, $6H_2O$) and copper nitrate $Cu(NO_3)_2$, $3H_2O$). The atomic percentage of [Co-Cu] varied as 1.5 %, 2 %, 3 %, 5 %, and 7 %. The solution was dropped onto the heated substrates and allowed to remain at the optimal surface temperature (400 °C). For all experiments, the distance between the nozzle and the surface being studied (25 cm) was kept constant.

The structural properties of $Zn_{1-(0.02+y)}Co_{0.02}Cu_yO$ thin films were investigated using diffraction by X-rays (XRD Bruker AXS-8D) under CuKα radiation ($\lambda$ = 1.5406 Å) within examining range 2 from 20° to 90°.The transparency of the deposited films was determined through an ultraviolet-visible spectrophotometer (LAMBDA 25) in the wavelength range of 300 nm - 1200 nm.

## Results and discussion

The XRD spectra of spray pyrolysis-fabricated Co and Cu co-doped ZnO thin films are shown in Figure 1. The Co and Cu co-doped ZnO thin films were deposited at various atomic concentrations [Co-Cu] (1.5 %, 2 %, 3 %, 5 %, and 7 %). Hexagonal ZnO (wurtzite, JCPDS 36-1451) was used to compare the detected peaks. We have observed from XRD diffraction peaks various diffraction peaks such as (100), (002), and (101) planes, which found by many authors [16-18]. In each of the samples, the observations revealed three diffraction peaks, the greatest being at $2\theta$ = 31.6°, $2\theta$ = 34.42°, and $2\theta$ = 36.10°, and matching to the following plans (100), (002) and (101), respectively, which are demonstrated by Diha et al. [19] and Cao and Bai [20]. However, we have found another phase 7 % Cu related to the CuO due to the Cu levels.  The best result was found with $Zn_{0.985}Co_{0.02}Cu_{0.015}O$ and $Zn_{0.96}Co_{0.02}Cu_{0.02}O$.

The lattice parameters of *a* and *c* of Co and Cu codoped ZnO thin films were measured according the (100) and (002) planes using the following formula [21, 22]:

$$d_{hkl} = \frac{a}{\sqrt{\frac{4}{3}\left(h^2 + k^2 + hk\right) + l^2 \frac{a^2}{c^2}}} \quad (1)$$

where $d_{hkl}$ is the interplanery and ($hkl$) is Miller indices, Table 1 presents the measured values. However, the crystallite size $D_{hkl}$ of sprayed thin films was calculated by the Debye-Scherrer equation [23]:

$$D_{hkl} = \frac{k\lambda}{\beta_{hkl}\cos\theta} \tag{2}$$

where $\beta_{hkl}$ is the full width at half-maximum (FWHM), $k$ is a constant real equal to 0.90, $\lambda$ is the incident wavelength X-ray ($\lambda$ = 0.15406 nm) and $\theta$ is the Bragg angle.

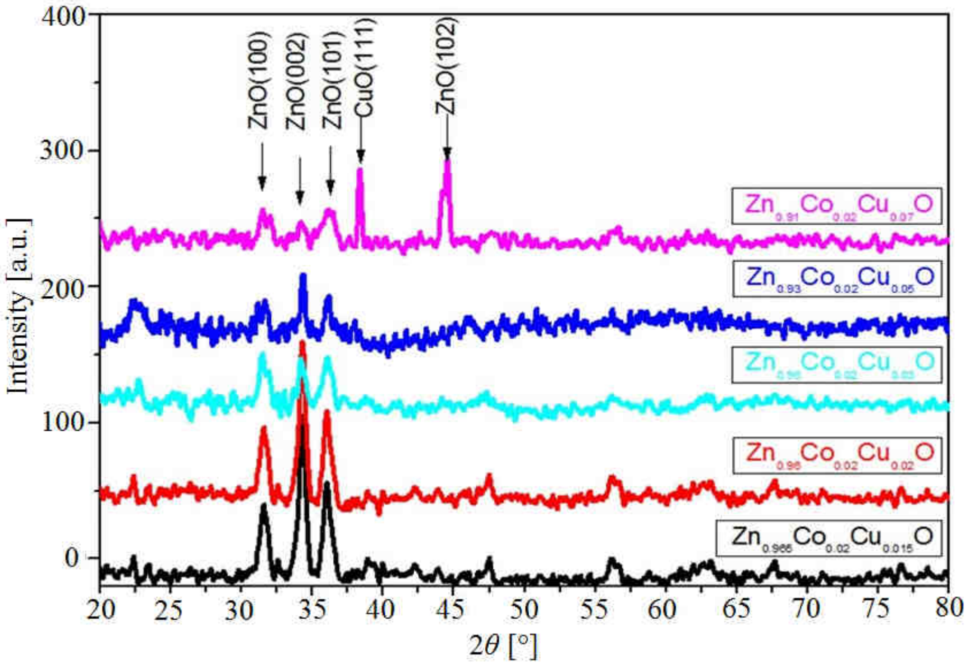


Fig. 1. X-ray diffraction spectra of fabricated $Zn_{1-(0.02+y)}Co_{0.02}Cu_yO$ thin films

Figure 2 and Table 1 present the measured variations of the lattice parameter $c$ and the average crystallite size of the Co- and Cu-doped ZnO thin films. Accordingly, as Cu levels increased, the average crystallite size decreased to a minimum value of 14.67 nm, as explained by the Co-Cu-Zn corporations. However, as Cu levels increased, the lattice parameter $c$ shifted twice towards two different values. Furthermore, when Cu ions and Co ions were doped, all of the diffractive peaks in the XRD patterns shifted to the lower angle side because the ionic radius of $Cu^{2+}$ (0.95 Å) and $Co^{3+}$ (0.58 Å) was greater than that of $Zn^{2+}$ (0.60 Å). Additionally, when Cu ions are doped, the peak intensity decreases, indicating that the crystalline quality deteriorates. According to the XRD results, Cu ions are successfully doped into the ZnCoO crystal structure with Zn ion substitution sites [21-26].

Table 1

Variation of lattice parameters *a* and *c*, and the average crystallite size $D_m = \frac{D_{(100)}+D_{(002)}+D_{(101)}}{3}$ of $Zn_{1-(0.02+y)}Co_{0.02}Cu_yO$ thin films

| Sample | *a* [Å] ± 0.0001 Å | *c* [Å] ± 0.0001 Å | Average crystallite size $D_m$ [nm] ± 0.01 nm |
|---|---|---|---|
| $Zn_{0.965}Co_{0.02}Cu_{0.015}O$ | 3.2737 | 5.2256 | 31.82 |
| $Zn_{0.94}Co_{0.02}Cu_{0.02}O$ | 3.2738 | 5.2257 | 29.76 |
| $Zn_{0.95}Co_{0.02}Cu_{0.03}O$ | 3.2812 | 5.2421 | 29.34 |
| $Zn_{0.93}Co_{0.02}Cu_{0.05}O$ | 3.2804 | 5.2168 | 27.42 |
| $Zn_{0.91}Co_{0.02}Cu_{0.07}O$ | 3.2739 | 5.2314 | 14.67 |

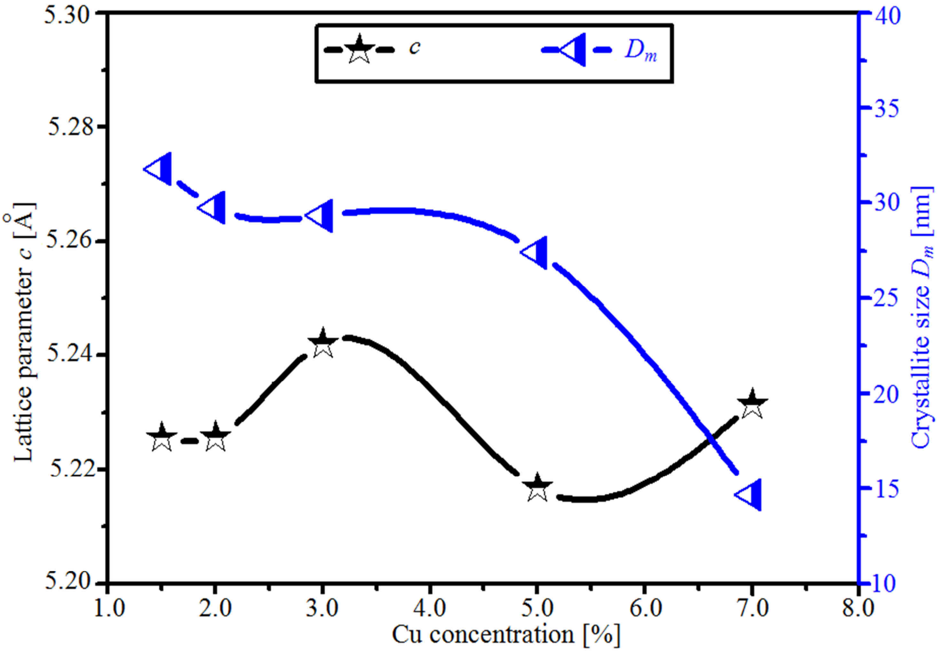


Fig. 2. The variations of lattice parameter c and average crystallite size $D_m$ of $Zn_{1-(0.02+y)}Co_{0.02}Cu_yO$ thin films

Figure 3 shows the transmission spectra of produced $Zn_{1-(0.02+y)}Co_{0.02}Cu_yO$ thin films created at various atomic percentages of Cu. There was an average measuring transmittance of 75 % - 85 % in the region of visible. Upon increasing the Cu doping levels, the optical transmittance spectra exhibited a red shift in the region of 300 and 400 nm. All films exhibit a significant rise in transmittance. The transmittance of all films reduced suddenly between 300 and 400 nm due to the fundamental absorption edge caused by the transition between the valence band and conduction band. This edge is used to compute the film optical band gap $E_g$, which is measured by the following relationships [27, 28]:

$$A = \alpha d = -\ln T \tag{3}$$

$$\left(Ah\upsilon\right)^2 = C\left(h\upsilon - E_g\right) \tag{4}$$

where $A$ is the absorbance of sprayed thin films, $\alpha$ is the coefficient of absorption, $T$ is the transmission of sprayed thin films, $C$ is a constant, $d$ is the film thickness, $h\upsilon$ is the photon energy [eV] $h\upsilon = 1240/\lambda$. However, the following equation was used to determine the disorder or Urbach energy $E_u$ [26, 27]:

$$A = A_0 \exp\left(\frac{h\upsilon}{E_u}\right) \tag{5}$$

where $A_0$ is a constant. The measured values of $E_g$ and $E_u$ are presented in Table 2.

Table 2

Variation of optical bandgap energy $E_g$ and Urbach energy $E_u$ of $Zn_{1-(0.02+y)}Co_{0.02}Cu_yO$ thin films

| **Sample** | **$E_g$ [eV] ± 0.01 eV** | **$E_u$ [eV] ± 0.01 eV** |
|---|---|---|
| $Zn_{0.965}Co_{0.02}Cu_{0.015}O$ | 3.35 | 0.31 |
| $Zn_{0.94}Co_{0.02}Cu_{0.02}O$ | 3.50 | 0.27 |
| $Zn_{0.95}Co_{0.02}Cu_{0.03}O$ | 3.48 | 0.28 |
| $Zn_{0.93}Co_{0.02}Cu_{0.05}O$ | 3.31 | 0.33 |
| $Zn_{0.91}Co_{0.02}Cu_{0.07}O$ | 3.46 | 0.29 |

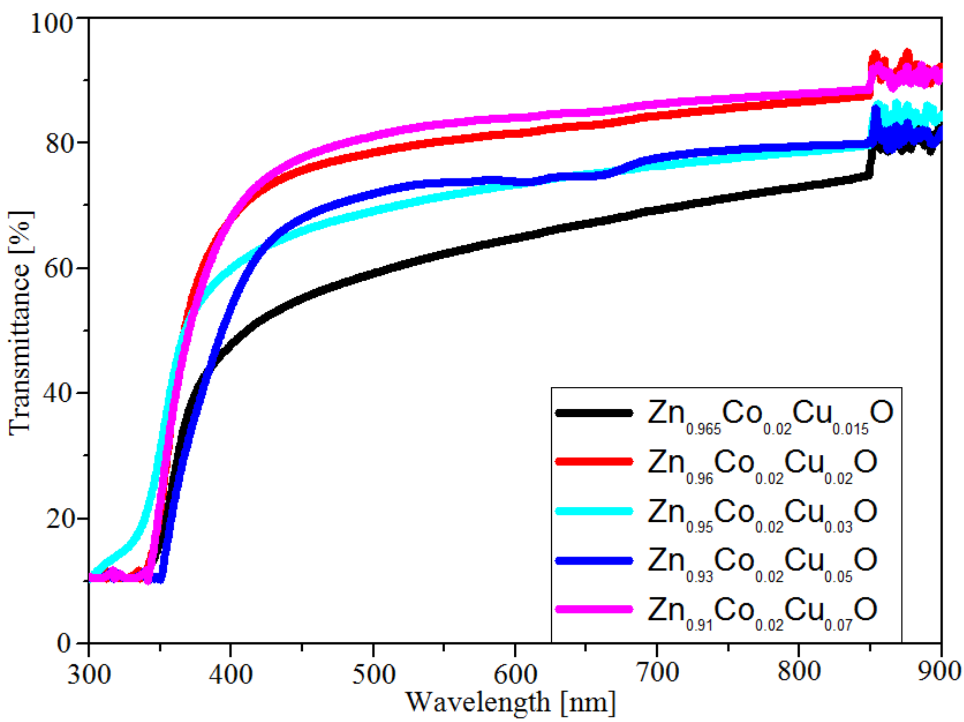


Fig. 3. Variation of transmittance spectra of sprayed $Zn_{1-(0.02+y)}Co_{0.02}Cu_yO$ thin films

The variation of optical gap energy and Urbach energy of the co-doping thin films of $Zn_{1-(0.02+y)}Co_{0.02}Cu_yO$ are shown in Figure 4. As the results showed, the thin film prepared with 2 % Co and 2 % Cu had minimal disorder of 0.27 eV with few defects. However, the optical gap energy increased from 3.35 eV to 3.50 eV then decreased from 3.50 eV to 3.31 eV with an increase of Cu concentration. This can be explained by the oxygen diffusion or the free oxygen due to the incorporation of Cu and Zn in the formation of CoCuZnO thin films. The results of the increase in the optical bandgap represent an important parameter of advanced materials and have potential applications for visible light as a gas sensor involving metal oxide nanostructures.

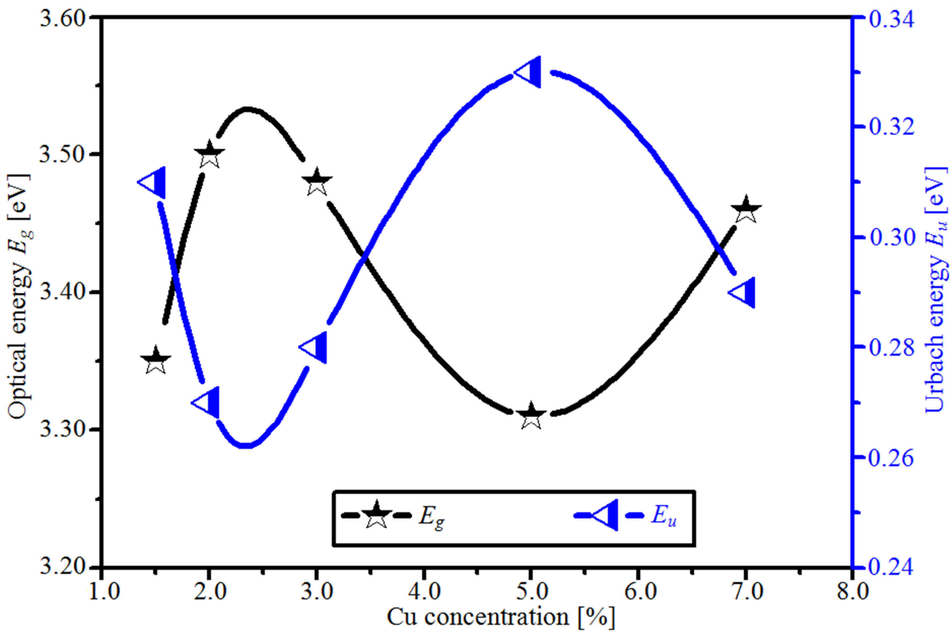


Fig. 4. The variation of optical band gap $E_g$ and Urbach energy $E_u$ of fabricated $Zn_{1-(0.02+y)}Co_{0.02}Cu_yO$ thin films

## Conclusion

In conclusion, the Co and Cu co-doped ZnO thin films were successfully elaborated on glass substrate by the spray pneumatic method at 400 °C. The thin films were obtained by combining zinc acetate ($Zn(CH_3CO_2)_2$, $2H_2O$) in distilled water to form a 0.1M solution with cobalt chloride ($CoCl_2$, $6H_2O$) and copper nitrate ($Cu(NO_3)_2$, $3H_2O$). The influence of various Co and Cu levels on the crystalline structure, transmittance, and optical energy of Co and Cu co-doped ZnO thin films has been investigated. The X-ray diffraction patterns of the Co and Cu co-doping ZnO thin films showed that the obtained thin films are hexagonal ZnO (wurtzite, JCPDS 36-1451). The minimum value of average crystallite size of 14.67 nm was observed for 2 % Co and 7 % Cu. The transmission spectra show that the Co and Cu co-doping ZnO thin films have good optical transparency in the region of visible with high transmission was obtained for 7 % Cu. The high optical gap energy is 3.50 eV obtained for 2 % Co and 2 % Cu. And the minimum value was 3.31 eV obtained for 2 % Co and 5 % Cu. The results of the increase in the optical bandgap represent an important parameter of advanced materials and have potential applications for visible light as a gas sensor involving metal oxide nanostructures.

## References

[1] Asikuzun E, Ozturk O, Arda L, Terzioglu C. Preparation, growth and characterization of nonvacuum Cu-doped ZnO thin films. J Mol Struct. 2018;1165:1-7. DOI: 10.1016/j.molstruc.2018.03.053.

[2] Akcan D, Gungor A, Arda L. Structural and optical properties of Na-doped ZnO films. J Mol Struct. 2018;1165:299-305. DOI: 10.1016/j.molstruc.2018.02.058.

[3] Ammaih Y, Abderrazak A, Hartiti B, Ridah A, Thevenin P, Siadat M. Structural, optical and electrical properties of ZnO:Al thin films for optoelectronic applications. Opt Quantum Electronic. 2014;46:229-34. DOI: 10.1007/s11082-013-9757-2.

[4] Heiba ZK, Arda L. XRD, XPS, optical, and Raman investigations of structural changes of nano Co-doped ZnO. J Mol Struct. 2012;1022:167-71. DOI: 10.1016/j.molstruc.2012.04.091.

[5] Benramache S. Fabrication and characterisation of ZnO thin film by sol-gel technique. Ann West Univ Timisoara-Phys. 2019;61:64-70. DOI: 10.2478/awutp-2019-0006.

[6] Althobaiti MG, Alharthi SS, Alharbi AN, Badawi A. Impact of silver/copper dual-doping on the structure, linear and non-linear optical performance of ZnO thin films. Appl Phys A. 2022;128:539. DOI: 10.1007/s00339-022-05682-y

[7] Kadari AS, Ech-Chergui AN, Aïssa B, Mukherjee SK, Benaioun N, Zakaria Y, et al. Growth and characterization of transparent vanadium doped zinc oxide thin films by means of a spray pyrolysis process for TCO application. J Sol-Gel Sci Technol 2022;103:691-703. DOI: 10.1007/s10971-022-05875-0

[8] Benramache S, Chabane F, Arif A. The deposition temperature dependence on the crystallite size of NiO thin films. Materials Geoenviron. 2020;67:35-8. DOI: 10.2478/rmzmag-2020-0001.

[9] Mohaseba MA, Aboud AA. Effect of Pb doping onto physical properties of ZnO thin films deposited by AACVD. J Mater Sci: Mater Electron. 2023;34:941. DOI: 10.1007/s10854-023-10360-7.

[10] Alqadi MK, Migdadi AB, Alzoubi FY, Al-khateeb HM, Almasri AA. Influence of (Ag-Cu) co-doping on the optical, structural, electrical, and morphological properties of ZnO thin films. J Sol-Gel Sci Technol. 2022;103:319-34. DOI: 10.1007/s10971-022-05785-1

[11] Guler A, Arda L, Dogan N, Boyraz C, Ozugurlu E. The annealing effect on microstructure and ESR properties of (Cu/Ni) co-doped ZnO nanoparticles. Ceram Int. 2019;45:1737-45. DOI: 10.1016/j.ceramint.2018.10.056.

[12] Boyraz C, Dogan N, Arda L. Microstructure and magnetic behavior of (Mg/Ni) co-doped ZnO nanoparticles. Ceram Int. 2017;43:15986-91. DOI: 10.1016/j.ceramint.2017.08.184.

[13] Yatskiv R, Grym J, Bašinová N, Kučerová Š, Vaniš J, Piliai L, et al. Defect-mediated energy transfer in ZnO thin films doped with rare-earth ions. J Lumin. 2023;253:119462. DOI: 10.1016/j.jlumin.2022.119462.

[14] Kumar P, Nisha Sarkar P, Sarkar P, Singh S, Mishra BCK, Katiyar RS. The influence of post-growth heat treatment on the optical properties of pulsed laser deposited ZnO thin films. Appl Phys A. 2022;128:372. DOI: 10.1007/s00339-022-05511-2.

[15] Souad D, Benramache S, Ammari A, Gahtar A. Effect of substrate temperature on the structural, optical, electrical, and morphological properties of zinc oxide thin films, Iranian J Phys Res. 2022;22:85-91. DOI: 10.47176/ijpr.22.3.01590.

[16] Orelusi AN, Owoeye VA, Dada JB, Salau AO, Boyo HO, Adewinbi SA. Investigation of microstructure and optical characteristics of Ti-doped ZnO thin films as an effective solar collector in photovoltaic solar cell applications using digitally controlled spray pyrolysis. J Materials Res. 2023;38:4192-200. DOI: 10.1557/s43578-023-01133-3.

[17] Bouachiba Y, Mammeri A, Bouabellou A, Rabia O, Saidi S, Taabouche A et al. Optoelectronic and birefringence properties of weakly Mg-doped ZnO thin films prepared by spray pyrolysis. J Mater Sci: Mater Electron. 2022;33:6689-99. DOI: 10.1007/s10854-022-07844-3.

[18] Li Z, Xiao W, Zhou H, Shi Z, Li L, Zhang J et al. Preparation and photoelectric properties of silver nanowire/zno thin film ultraviolet detector. Electron Mater Lett. 2023;19:415-23. DOI: 10.1007/s13391-023-00421-8

[19] Diha A, Benramache S, Benhaoua B. Transparent nanostructured Co doped NiO thin films deposited by sol-gel technique. Optik. 2018;172:832-9. DOI: 10.1016/j.ijleo.2018.07.062.

[20] Cao P, Bai Y. Structural and electrical properties of (Cu, Co) co-doped ZnO thin film. Adv Mater Res. 2013;774-776:964-7. DOI: 10.4028/www.scientific.net/AMR.774-776.964.

[21] Zhao JL, Sun XW, Ryu H, Moon YB. Thermally stable transparent conducting and highly infrared reflective Ga-doped ZnO thin films by metal organic chemical vapor deposition. Optical Mater. 2011;33:768-72. DOI: 10.1016/j.optmat.2010.12.008.

[22] Benramache S, Aoun Y, Lakel S, Mourghade H, Gacem R, Benhaoua B. Effect of annealing temperature on structural, optical and electrical properties of ZnO thin films prepared by sol-gel method. J. Nano Electron Phys. 2018;10:06032. DOI: 10.21272/jnep.10(6).06032.

[23] Chehhat K, Mecif A, Mahdjoub AH, Andrabi RN, Pandit MA, Salhi FF, et al. Sol-gel synthesis of porous cobalt-doped ZnO thin films leading to rapid and large scale Orange-II photocatalysis. J Sol-Gel Sci Technol. 2023;106:85-94. DOI: 10.1007/s10971-023-06060-7

[24] Smith RMS, Amiri M, Martin NP, Lulich A. Palys LN, Zhu G, et al. Solvent-driven transformation of Zn/Cd2+-deoxycholate assemblies. Inorg Chem. 2022;61:1275-86. DOI: 10.1021/acs.inorgchem.1c02245.

[25] Meelua W, Oláh J, Jitonnom J. Role of water coordination at zinc binding site and its catalytic pathway of dizinc creatininase: insights from quantum cluster approach. J Comput Aided Mol Des. 2022;36:279-89. DOI: 10.1007/s10822-022-00451-8.

[26] Ech-Chergui AN, Kadari AS, Khan MM, Popad A, Kane Y, Guezzoul M et al. Spray pyrolysis-assisted fabrication of Eu-doped ZnO thin films for antibacterial activities under visible light irradiation. Chem Pap. 2023;77:1047-58. DOI: 10.1007/s11696-022-02543-z.

[27] Meryem LZ, Touidjen NEH, Aida MS, Aouabdia N, Rouabah S. Growth of undoped ZnO thin films by spray pyrolysis: effect of precursor concentration. J Opt. 2023;52:1782-8. DOI: 10.1007/s12596-022-01079-5.